preciably with the remaining alkyl protons of the molecule. Thus, differential development of proton spin coherence can be distinguished (in this case) for *different* segments of the *same* molecule. The higher order ($n > 2$) coherences in Figure 5B do not grow much even for longer preparation times, and we regard their presence primarily as artifacts arising from imperfect discrimination between multispin clusters and nearly isolated spin pairs by the solid echo sequence, rather than a leakage of order to other parts of the molecule.

The observed MQ intensities, without solid echo selection, can now be analyzed since we have evidence that the overall spin system is a superposition of a small, primarily two-spin subsystem, with a larger, more weakly coupled system from the alkyl chain protons. We model the intensity of the n-order coherence in the (nonselective) MQ spectrum as a superposition of a Gaussian for the larger subsystem and a two spin system

$$I_{obs_{ns}}[n(\tau)] = M_g \exp[-n(\tau)^2/N_e] + M_2[\delta(0) + \delta(2)] \quad (5a)$$

where $\delta(0)$ and $\delta(2)$ represent the intensities of the zero- and two-quantum coherences due to the two-spin subsystems, and N_e is the effective system size for the larger subsystem. There are also some normalization factors (M_g and M_2) to be accounted for. For the solid echo selected MQ sequence, we would expect M_g to be zero in eq 5, provided the solid echo selection worked perfectly. These contributions of the higher order coherences to the solid echo selected MQ spectrum are small though not zero, cf. Figure 5b, and the details of how they are handled do not affect the general conclusions. We allow a fraction (ϵ) of the Gaussian to persist:

$$I_{obs_{ss}}[n(\tau)] = c([\epsilon M_g \exp[-n(\tau)^2/N_e] + M_2[\delta(0) + \delta(2)]]) \quad (5b)$$

Here c is a constant describing the efficiency of the solid echo sequence relative to eq 5a. Note that in these experiments the zero-order coherence is not recorded.

At each preparation time, analysis proceeds by fitting the $n > 2$ coherences of the nonselective MQ spectrum to the Gaussian in eq 5a, determining the two-spin contribution to the two-quantum coherence, and then extracting ϵ from eq 5b. ϵ is found to be more or less independent of the preparation time τ, indicating that the higher order coherences in the solid echo selected MQ spectrum are indeed due to the inefficiency of the solid echo selection and do not come predominantly from two spin systems. Experimental MQ data and a representative fit are shown in Figure 6.

The number of spins which are in the two-spin system can now be calculated: (i) the number of spins in the N spin system and its integrated intensity, I_g, (over all coherences) is known. The integrated intensity, I_2, of the two-spin system can also be calculated by noting that the zero- and two-quantum intensities are equal (eq 2) and then the number of protons in the two-spin systems is calculated as $N_2 = (I_2/I_g)^*N$.

We find that over a wide range of preparation times ($10 \leq \tau/\tau_C \leq 60$), $N = 13 \pm 1$, and from the ratio of M_g/M_2 and appropriate normalizations for the Gaussian and two-spin systems, there are eight protons in two-spin systems for every 13-spin system. This result is consistent with the structure of the liquid crystal mixture: for the "average" molecule there are eight phenyl protons and 15 and 9 alkyl protons, in a 2:1 ratio, respectively. If these two respective Gaussians are not resolved, we should expect a single Gaussian with an effective size of 13.3 spins, quite close to our result of 13 ± 1.

Conclusions

The development of MQ coherence is the result of the concerted interaction of numerous spins in a solid. The development is dynamic and is first dominated by the largest couplings present. While all spins would in principle be affected by every spin present, we have presented a case where the distance separating spins can actually isolate collections or intramolecular clusters as seen in the data presented. Furthermore, the differential relaxation properties (in this case, T_2 and the special properties of two-spin dipolar couplings) of a molecule may be effectively utilized to focus upon and distinguish groups of nuclei within a molecule where their contributions to the overall development of MQ coherence are limited by their geometry, internal motions, or separation from other dipolar species. We have employed a highly simplified model to account for the gross features of the MQ development of the two subsystems, the alkyl chain protons, and sets of spin pairs on the phenyl head groups.

Solid-State Voltammetry and Self-Diffusion Dynamics of a Linear Monotagged Redox Polymer: ω-Ferrocenecarboxamido-α-methoxypoly(ethylene oxide)

M. J. Pinkerton, Y. Le Mest,† H. Zhang, M. Watanabe,‡ and Royce W. Murray*

Contribution from the Kenan Laboratories of Chemistry, University of North Carolina, Chapel Hill, North Carolina 27599-3290. *Received November 6, 1989*

Abstract: The synthesized title labeled polymer, Fc-MePEG, MW = 2590, analytically characterized as free of unlabeled PEO and of ferrocene monomer, dissolves $LiClO_4$ electrolyte and in dry undiluted form is both a polymer electrolyte and an electroactive phase. The microelectrode solid-state voltammetrically measured, center-of-mass self-diffusion coefficient for Fc-MePEG in its polymer melt, 1.3×10^{-8} cm^2/s at 62 °C, is 3.4 times smaller than that for ferrocene monomer dissolved in unlabeled (MW = 2380) Me_2PEG. Electron hopping is estimated to contribute less than 10% to the diffusion rates of Fc-MePEG and of monomer dissolved at 40–50 mM concentrations in unlabeled Me_2PEG. At room temperature, where Fc-MePEG and Me_2PEG are waxy solids, $D_{Fc\text{-}MePEG}$ is 3.9×10^{-12} cm^2/s, 12 times smaller than that of monomer ferrocene, in Me_2PEG, and which corresponds to a diffusion pathlength of ca. 110–200 nm during the electrochemical experiment. Dissolved in CH_3CN or CH_2Cl_2, Fc-MePEG diffuses 8–10 times more slowly than ferrocene monomer which is consistent with transport as a random coiled sphere.

This paper describes the voltammetric determination of the center-of-mass self-diffusion coefficient of a linear polymer chain bearing a single redox end group (ferrocene), in the pure polymer phase, and as a polymer solution in unlabeled polymer of similar MW. ω-Ferrocenecarboxamido-α-methoxypoly(ethylene oxide), $CpFeCpCONH(CH_2CH_2O)_nCH_3$ (Fc-MePEG), was synthesized[1]

†Current address: U.A. C.N.R.S. 322, Departement de Chimie, Universite de Bretagne Occidentale, 6 Avenue Le Gorgeu, 29287 Brest, Cedex, France.
‡Permanent address: Department of Chemistry, Sophia University, 7-1 Kioi-cho, Chiyoda-ku, Tokyo 102, Japan.

(1) Zalipsky, S.; Gilon, C.; Zilkha, A. *Eur. Polym. J.* **1983**, *19*, 1177.

0002-7863/90/1512-3730$02.50/0

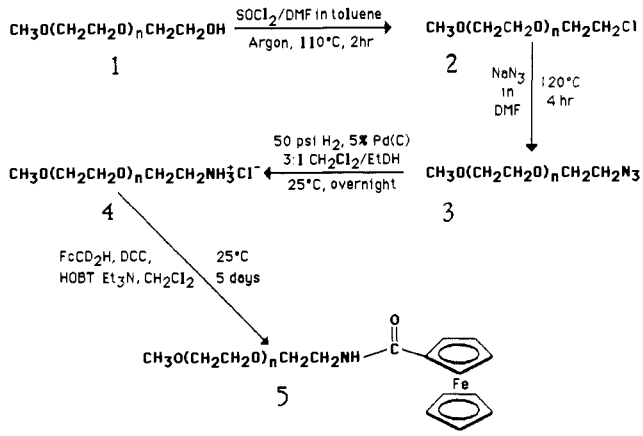

Figure 1. Reaction scheme for the synthesis of Fc-MePEG, **5**.

and analytically characterized as free of unlabeled ferrocene. Analogous to poly(ethylene oxide),[2] Fc-MePEG dissolves lithium salts and, as a pure phase or diluted with unlabeled $CH_3O(CH_2CH_2O)_nCH_3$, (Me_2PEG), serves as a solid-state, electrochemically reactive polymer electrolyte. Having recently demonstrated[3] quantitative electrochemical voltammetry of monomer redox solutes in solid polymer electrolytes, we apply this microelectrode-based methodology to measure the self-diffusion rates of ferrocene-labeled polymer chain Fe-MePEG in itself and as a solute in unlabeled polymer Me_2PEG. The polymer chain diffusion coefficient $D_{Fc\text{-}MePEG}$ ranges from 3.3×10^{-8} cm^2/s at 89 °C in the melt state to 4×10^{-12} cm^2/s at room temperature (waxy solid). The $D_{Fc\text{-}MPEG}$ results are compared to diffusion coefficients of the monomeric redox label, ferrocene, in unlabeled polymer Me_2PEG and in fluid solvents.

Additional motivations for the present study were as follows. (i) The insufficient solubility of many interesting redox species in solid PEO solvents should be corrected by attaching poly(ethylene oxide) appendages.[1,4] PEO tails are known to confer aqueous solubility on a wide range of chemical species.[4] Remarkably, Fc-MePEG is soluble both in toluene and in water. (ii) There have been few reports[5,6] of electrochemical voltammetry of polymers bearing restricted numbers of redox groupings per polymer chain; this is the first on a polymer with a *single*, well-defined, redox grouping. (iii) The development of reptation theory[7] connecting self-diffusion rates to molecular weights of linear polymers gives special value to new experimental approaches to polymer self-diffusion rates. Existing methods[8,9] include fluorescence redistribution following pattern photobleaching which has been applied to the related polymer, poly(propylene oxide).[9] Electrochemical measurement of polymer self-diffusion has not been previously reported and appears to offer an exceptional dynamic range for center-of-mass self-diffusion, from $>10^{-8}$ to 3×10^{-12} cm^2/s in the present data.

Diffusion coefficients in polymeric phases are often composition-dependent, so a careful analytical characterization of the synthesized Fc-MePEG was conducted. Fc-MePEG in water, acetonitrile, and dichloromethane gave normal ferrocene voltammetry apart from a slowed diffusion rate. Finally, the diffusion rates of solvent free Fc-MePEG and of ferrocene monomer are compared, and the possible contribution of electron self-exchange dynamics to the overall Fc-MePEG and ferrocene transport dynamics is estimated.

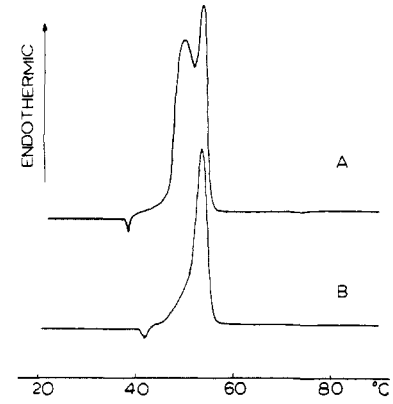

Figure 2. Differential scanning calorimetry of Fc-MePEG, **5**: (A) crude product and (B) purified product.

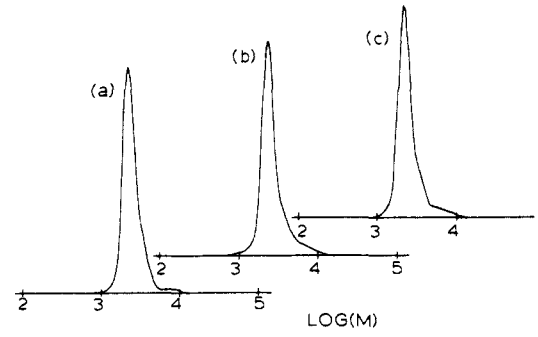

Figure 3. Molecular weight distribution curves of Me_2PEG and Fc-MePEG polymers determined from GPC elution curves and a molecular weight calibration curve based on PEG standards: (A) Me_2PEG (**1**) detected by RI, (B) Fc-MePEG (**5**) detected by RI, (C) Fc-MePEG (**5**) detected by UV–vis at 438 nm.

Results and Discussion

Synthesis, Purification, and Characterization. The synthetic pathway (Figure 1, details in Experimental Section), based on previous chemistry by Zalipski, et al.,[1] was refined aiming at analytically pure material for transport measurements. Commercial monomethyl poly(ethylene glycol) MePEG, **1**, was chlorinated (MePEG-Cl, **2**), converted to the monoazide MePEG-N_3, **3**, hydrogenated to the amine salt MePEG-NH_3^+, **4**, and coupled to ferrocene carboxylic acid to give a crude Fc-MePEG product, **5**. This material exhibited the expected ferrocene amide carbonyl stretch at 1649 cm^{-1} but also impurity[1] bands at 3324 cm^{-1} (ν_{NH}, **4**) and 669 cm^{-1} (ν_{CCl}, **2**). Differential scanning calorimetry (Figure 2A) also indicates a polymeric impurity; the two endotherms at 50 °C (broad) and 53.7 °C (sharp), both occur at typical poly(ethylene glycol) melting temperatures (T_m). Elemental Fe analysis of crude **5** gave result 80–90% of the ideal value, based on a Fc-MePEG number average molecular weight (M_n) of 2590 (vide infra GPC measurements), and cyclic voltammetry of crude **5** in $CH_3CN/LiClO_4$ exhibits an irreversible peak at 1.1 V in addition to the expected ferrocene/ferrocenium wave at +0.57 V vs Ag (ΔEp = 77 mV).

(2) (a) Ratner, M. A.; Shriver, D. F. *Chem. Rev.* **1988**, *88*, 109. (b) Armand, M. B. *Ann. Rev. Mater. Sci.* **1986**, *16*, 245. (c) Vincent, C. A. *Solid State Chem.* **1987**, *17*, 145. (d) Watanabe, M.; Ogata, N. *Brit. Polymn. J.* **1988**, *20*, 181.

(3) (a) Geng, L.; Reed, R. A.; Kim, M. H.; Wooster, T. T.; Oliver, B. N.; Egekeze, J.; Kennedy, R. T.; Jorgenson, J. W.; Parcher, J. W.; Murray, R. W. *J. Am. Chem. Soc.* **1989**, *111*, 1614. (b) Geng, L.; Longmire, M. L.; Reed, R. A.; Parcher, J. F.; Barbour, C. J.; Murray, R. W. *Chem. Mater.* **1989**, *1*, 58. (c) Oliver, B. N.; Egekeze, J. O.; Murray, R. W. *J. Am. Chem. Soc.* **1988**, *110*, 2321. (d) Geng, L.; Reed, R. A.; Longmire, M.; Murray, R. W. *J. Phys. Chem.* **1987**, *91*, 2908. (e) Reed, R. A.; Geng, L.; Murray, R. W. *J. Electroanal. Chem.* **1986**, *208*, 185.

(4) (a) Mutter, M.; Altmann, K. H.; Gehrhardt, H. *Reactive Polymers* **1987**, *6*, 99. (b) Harris, J. M. *JMS-REV., Macromol. Chem. Phys.* **1985**, *C25*, 325. (c) Aida, T.; Takemura, A.; Fuse, M.; Inoue, S. *J. Chem. Soc., Chem. Commun.* **1988**, 391. (d) Kodera, Y.; Ajima, A.; Takahashi, K.; Matsushima, A.; Saito, Y.; Inada, Y. *Photochem. Photobiol.* **1988**, *47*, 221. (e) Takahashi, K.; Matsushima, A.; Saito, Y.; Inada, Y. *Biochem. Biophys. Res. Commun.* **1986**, *138*, 283.

(5) Kuhn, L. S.; Weber, S. G.; Ismail, K. Z. *Anal. Chem.* **1989**, *61*, 303.

(6) Margerum, L. D.; Meyer, T. J.; Murray, R. W. *J. Phys. Chem.* **1986**, *90*, 2696.

(7) (a) de Gennes, P.-G. *Scaling Concepts in Polymer Physics*; Cornell University Press: Ithaca, NY, 1979. (b) Doi, M.; Edwards, S. F. *The Theory of Polymer Dynamics*; Oxford University Press: New York, 1986.

(8) Tirrell, L. *Rubber Chem. Technolog.* **1984**, *57*, 523.

(9) (a) Smith, B. A.; Mumby, S. J.; Samulski, E. T.; Yu, L. P. *Macromolecules* **1986**, *19*, 470. (b) Smith, B. A.; Samulski, E. T.; Yu, L. P.; Winnik, M. A. *Macromolecules* **1985**, *18*, 1901. (c) Smith, B. A.; Samulski, E. T.; Yu, L. P.; Winnik, M. A. *Phys. Rev. Lett.* **1984**, *52*, 45.

Table I. Molecular Weight Data Obtained by Gel Permeation Chromatography

sample	M_n[a]	M_w[b]	M_w/M_n
Me_2PEG (RI)[c]	2380	2590	1.09
Fc-MePEG (RI)[c]	2460	2780	1.13
Fc-MePEG (UV-vis)[d]	2430	2750	1.14

[a] Number average molecular weight. [b] Weight average molecular weight. [c] Molecular weight data are determined by using an RI detector. [d] Molecular weight data are determined by using a UV-vis detector set at 438 nm.

The differences in hydrophobicity between Fc-MePEG and its precursors sufficed for purification by hydrophobic interaction chromatography on a phenylsepharose column. FTIR of purified **5** lacks detectable bands for MePEG-Cl or MePEG-NH_3^+, and the sharp DSC endotherm (Figure 2B) at 53.7 °C exhibits only a small shoulder on the lower temperature side. ^{13}C NMR in $CDCl_3$ shows peaks for terminal methoxy (58.2 ppm), methylene β and α to amide nitrogen (67.6 and 38.4 ppm), aromatic ferrocene carbons (75.9, 76.2, and 76.4 ppm), and internal polymer methylenes (complex peak at 69.7 ppm) and lacks resonances indicative of terminal hydroxy (C_α 41.8, C_β 7.35 ppm),[10a] terminal amino (C_α 41.8, C_β 73.5 ppm),[10a] and terminal chloride (C_α 43.0, C_β 71.2 ppm).[10b] Repeated elemental analyses gave a %Fe that is 86% of the ideal value (2.16% for M_n = 2590), but coulometric analysis of ferrocene (vide infra) was satisfactory.

Gel permeation chromatography of MePEG starting material **1** and of purified **5** is presented in Figure 3 as MW distribution curves, calculated from the GPC elution profiles after column calibration with high MW accuracy PEG standards. Figure 3A gives results for **1** detected by RI (refractive index), and Figure 3 (parts B and C) gives results for **5** detected by RI and by UV-vis at 438 nm where ferrocene but not MePEG absorbs. GPC of **4** (not reported) gave an abnormally long elution time compared with MePEG and **5**, presumably due to adsorption on the column. The MW distribution curves of MePEG and **5** show (by both detectors) no low MW impurities and no slowly eluting **4**. The RI and UV-vis-detected molecular weight profiles for Fc-MePEG are superimposable, consistent with full labeling of the MePEG polymer. The tail at higher MW (log(MW) = 3.7-3.8) appears to be a higher molecular weight (by ca. 2×) fraction than the main one and is present in **1** as well as **5**; it accounts for <10% of the sample. The FTIR, DSC, ^{13}C NMR, and electrochemical coulometry (vide infra, $n = 1.2 \pm 0.1$) results collectively support a high purity level in terms of absence of nontagged MePEG polymer and of low molecular weight impurities. The absence of ferrocene monomer is particularly significant in regard to the transport measurements.

The GPC molecular weight (Table I), M_n = 2380, for starting material MePEG, **1**, is larger than the vendor's MW = 1900 value; we adopted our GPC result for calculations in the present work. The GPC M_n = 2460 result (by RI) for labeled molecule Fc-MePEG (**5**) (Table I) is possibly affected by the presence of the ferrocene moiety, relative to that of the poly(ethylene glycol) standards used for molecular weight calibration, so we calculated the Fc-MePEG molecular weight by adding that of ferrocene carboxyl to the determined parent MePEG MW (2380). The resulting value, 2590, was used in calculations of Fc-MPEG stoichiometry and concentrations.

We note that the two detectors give the same Fc-MePEG M_n, M_w, and polydispersity, M_w/M_n, Table I, and that the molecular weight dispersity, M_w/M_n = 1.13-1.14, is sufficiently narrow for meaningful transport measurements.

Solid-State Voltammetry of Polymer Phases. Cyclic voltammetry of the Fc/Fc^+ couple at a 10μ Pt microdisk[3,11,12] electrode

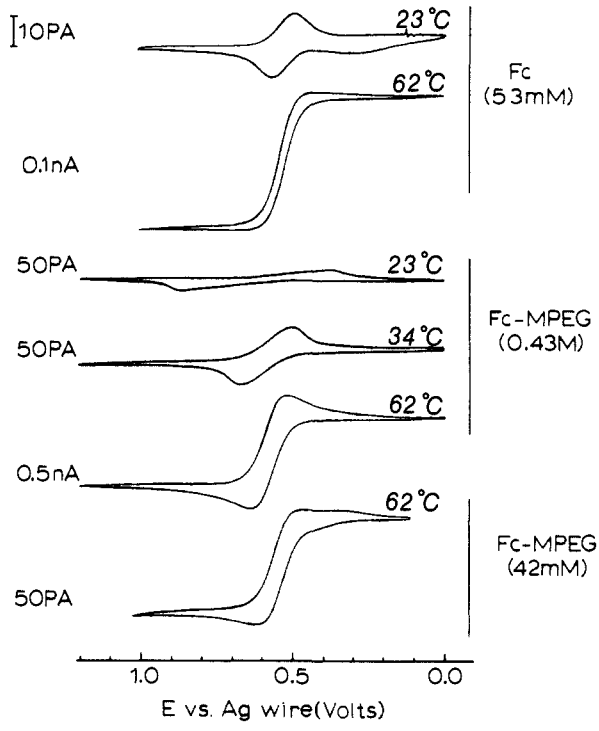

Figure 4. Cyclic voltammogram (5 mV/s) at a 10-μm microdisk electrode of polymer/$LiClO_4$ mixtures recorded at indicated temperatures: top, 53 mM ferrocene in Me_2PEG 2000; middle, bulk Fc-MePEG (0.43 M); bottom, 42 mM Fc-MePEG in Me_2PEG 2000. Ether oxygen/Li ratio = 16 throughout.

is shown in Figure 4 for three dry poly(ether) solutions, each containing $LiClO_4$ as electrolyte: (top) 53 mM ferrocene monomer dissolved in (unlabeled) Me_2PEG, (middle) undiluted Fc-MePEG ($C_{Fc\text{-}MePEG}$ = 0.43 M), and bottom 42 mM Fc-MePEG dissolved in (unlabeled) Me_2PEG. The temperatures shown span the polymer melting temperature (T_m = 53 °C, Figure 2B); the currents above T_m in the (highly viscous) polymer melt are much larger than those below T_m, where the polymer is a partly crystalline wax. Also, at 62 °C, the faster diffusion in the melts facilitates establishing radial diffusion profiles[12] at the microelectrode and, correspondingly, produces voltammetric waves with steady-state limiting currents and little hysteresis between positive and negative potential sweeps. The ferrocene monomer voltammetry gives larger currents and voltammograms with less hysteresis than do the Fc-MePEG solutions, indicating that Fc-MePEG diffuses more slowly. At temperatures below T_m, the diffusion geometry becomes more nearly linear as both monomer and polymer ferrocene diffuse more slowly in the partly crystalline polymer phases. Additionally, the polymers are much less (ionically) conductive at lower temperature, and the voltammograms become distorted by iR effects.

Identifying the diffusion geometry is necessary to properly extract diffusion coefficients from results like Figure 4. Diffusion coefficients at $T > T_m$ were determined from the voltammetric limiting currents (Figure 4) by using the equation[12]

$$i_{lim} = 4nrFD_{app}C \qquad (1)$$

where r is the microdisk electrode radius, D_{app} is the experimental (apparent) diffusion coefficient, and n, F, and C have their usual significance. At $T < T_m$, slower diffusion causes linear diffusion or mixed linear-radial diffusion, and diffusion coefficients were measured[13] from chronoamperometric current-time responses analyzed by, respectively, i vs $t^{-1/2}$ (Cottrell) plots[14] and comparisons to simulated current-time curves computed from mixed diffusion theory.[15] The details of measuring polymer phase

(10) (a) Ziegast, G.; Pfannemuller, B. *Polym. Bull.* **1981**, *4*, 467. (b) Compared to $ClCH_2CH_2OCH_2CH_2OH$, Sadtler Standard Carbon-13 NMR Spectra, Philadelphia, PA, 1976.

(11) The purpose of the microelectrode is to cause only small currents to flow, since the poly(ether) polymer electrolytes actually have only a small ionic conductivity.

(12) Wightman, R. M. *Anal. Chem.* **1981**, *53*, 1125A.

(13) Longmire, M. L.; Watanabe, M.; Zhang, H.; Wooster, T. T.; Murray, R. W. *Anal. Chem.* In press.

(14) Bard, A. J.; Faulkner, L. R. *Electrochemical Methods: Fundamentals and Applications*; Wiley: New York, 1981.

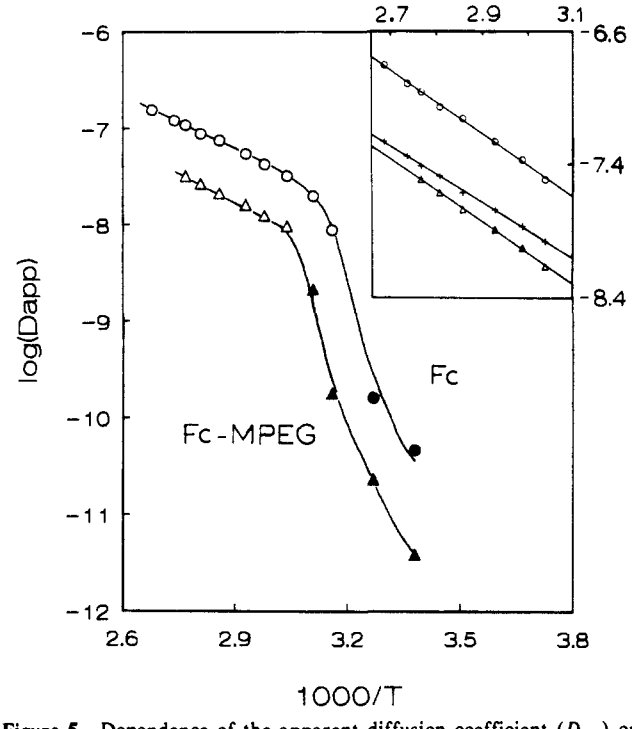

Figure 5. Dependence of the apparent diffusion coefficient (D_{app}) on temperature for 53 mM ferrocene in $Me_2PEG/LiClO_4$ (circles) and bulk Fc-MePEG/$LiClO_4$ (triangles) mixtures. Filled symbols are for chronoamperometrically determined values; empty ones are for those obtained by using eq 1. The inset is an enlargement of the temperature plots above T_m, and additional results for 42 mM Fc-MePEG diluted by $Me_2PEG/LiClO_4$ (+).

diffusion rates in radial, linear, and mixed diffusion regimes are given in an upcoming paper.[13]

The D_{app} results for the three polymeric media are summarized in Figure 5. The D_{app} temperature dependences in undiluted Fc-MePEG polymer electrolyte and for ferrocene monomer in Me_2PEG are qualitatively similar, including a sharp change in D_{app} at about 52 °C, corresponding to the DSC melting temperature, T_m = 53.8 °C, Figure 3. The inset shows Arrhenius plots above T_m, for undiluted Fc-MPEG(Δ), ferrocene monomer in Me_2PEG(O), and Fc-MPEG in Me_2PEG(+), which give diffusion activation barrier values E_a = 8.7, 8.7, and 7.8 kcal/mol, respectively. These results are considered ca. equal given the experimental uncertainty imposed by the proximity of the data to T_m.

The results in Figure 5 show that the transport barriers in the polymer melts differ by less than 1 kcal/mol whether ferrocene bears a polymer tail or not and that Fe-MePEG diffuses more slowly than monomer ferrocene by 3.4 times when $T > T_m$ and by *12* times at room temperature. In interpreting these results, we must consider the possibilities that (a) $D_{Fc\text{-}MePEG}$ mainly reflects the diffusivity of the ferrocene label, the intrinsic diffusivity of a Me-PEG chain being greater and thus nonlimiting, (b) $D_{Fc\text{-}MePEG}$ reflects the intrinsic diffusivity of an unlabeled MePEG polymer chain in an MePEG solvent, or (c) that the $D_{Fc\text{-}MePEG}$ and D_{Fc} reflect not physical diffusion but rather charge transport by electron self-exchange between ferrocene and ferricenium.

Choosing between interpretation (a) and (b) rests on judging whether, respectively, the presence of the ferrocene site slows down and dominates the diffusion of the polymer molecule Me-PEG, vs the diffusion of the Fc-PEG molecule being controlled by its polymer tail. In contrast to most polymer self-diffusion studies, we are able to explore this question by measuring the ferrocene diffusivity directly. In simple terms, if the diffusive mobility of ferrocene in unlabeled polymer Me_2PEG exceeds that of the label-bearing polymer chain Fc-MePEG in itself, a reasonable inference is that the intrinsic diffusive mobility (in a center-of-mass sense) of the label-bearing polymer chain Fc-MePEG is close to that of an unlabeled polymer chain, Me_2-PEG. This appears to be the case in the partly crystalline polymer at room temperature, where $D_{Fc\text{-}MePEG} \ll D_{Fc}$, and so we assert that $D_{Fc\text{-}MePEG}$ is a good measure of the *polymer chain* self-diffusion coefficient under those circumstances.

In the polymer melt, above T_m, on the other hand, while D_{Fc} is still larger, the difference between $D_{Fc\text{-}MePEG}$ and D_{Fc} is diminished to perhaps[16] only 3-fold. That is, the label-bearing PEO chain's mobility seems in this case to be only slightly less than that of the ferrocene label. As a consequence, while $D_{Fc\text{-}MePEG}$ *is* an exact measure of the self-diffusion of Fc-MePEG in Fc-MePEG, it should be taken as an *approximate* measure of the diffusion rate of an *un*labeled PEO chain in an MePEG environment of the same molecular weight. Previous self-diffusion measurements[9] of poly(propylene oxide) at a similar MW and of ferrocene carboxylic acid diffusion in network PEO[17] have in fact produced diffusion coefficients in the same range (10^{-8}–10^{-7} cm^2/s) as those for $D_{Fc\text{-}MePEG}$ in the melt interval in Figure 5.

The comparison between $D_{Fc\text{-}MePEG}$ and D_{Fc} in Figure 5 also provides clear evidence that the Fc-MePEG polymer self-diffuses in an extended as opposed to a coiled form. We have observed[17] that substituted ferrocene diffusion rates in network PEO polymer solvent depend on the diffusant steric bulk; for example, $CpFeCpCO_2H$ diffuses ca. 10 times faster than the more bulky decamethylferrocene, Cp^*_2Fe. Also, as shown below, when dissolved in fluid low molecular weight solvents, Fc-MePEG diffuses about 10-fold more slowly than does monomer ferrocene, a difference accountable by a random coil model. Given these two facts, the 3-fold difference between $D_{Fc\text{-}MePEG}$ and D_{Fc} is much too small to represent a diffusing coiled conformation of the Fc-MePEG polymer.

Interpretation (c) addresses the point that the diffusion of Fc-MePEG to the measuring microelectrode occurs in a boundary layer also containing outwardly diffusing Fc-MePEG$^+$. In such a *mixed-valent* solution, when physical diffusion is very slow and electron self-exchange rapid, the transport of electrochemical *charge* to the electrode can be augmented by electron hopping from Fc-MePEG to Fc-MePEG$^+$. The problem of mixed diffusion/electron hopping is expressed by the Dahms–Ruff relation[18]

$$D_{app} = D_{phys} + (\pi/4)\delta^2 C k_{app} \quad (2)$$

$$D_{app} = D_{phys} + (\pi/4)\delta^2 C[1/k_d + 1/k_{ex}]^{-1} \quad (3)$$

where δ is the center-to-center distance of the exchanging couple (7.6×10^{-8} cm for ferrocene), C is ferrocene concentration, D for Fc-MePEG and Fc-MePEG$^+$ are assumed equal, and k_{app} the apparent self-exchange rate constant is expressed as the true self-exchange rate constant, k_{ex}, and the collision-limited rate constant, k_d. The latter constant is connected to D_{phys} through the Smoluchowski equation.[19]

The results for D_{app} for ferrocene monomer and Fc-MePEG dissolved at nearly *equal concentrations* in Me_2PEG polymer solvent of varying temperture (Figure 5 inset) are usefully compared by eqs 2 and 3. For this purpose it is necessary to assume a literature result for k_{ex} and its dependence on temperature,[20] for both ferrocene monomer and Fc-MePEG; since k_{ex} is probably less in the polymer solvent (vide infra), this will have the effect of *over*estimating the electron-hopping contribution. Values for D_{phys} were calculated from eq 3 and expressed as a fractional

(15) Szabo, A.; Cape, D. K.; Tallman, D. E.; Dovach, P. M.; Wightman, R. M. *J. Electroanal. Chem.* **1987**, *217*, 417.

(16) An uncertainty in the D_{Fc} results is possible sublimation loss of ferrocene during the polymer solution preparation; such loss would cause us to *under*estimate D_{Fc}.

(17) Watanabe, M.; Longmire, M. L.; Murray, R. W. *J. Phys. Chem.* In press.

(18) (a) Dahms, H. *J. Phys. Chem.* **1968**, *72*, 362. (b) Ruff, I.; Friedrich, V. J. *Ibid.* **1971**, *75*, 3297. (c) Ruff, I.; Friedrich, V. J.; Csillag, K. *Ibid.* **1971**, *75*, 3303.

(19) (a) von Smoluchowski, M. *Phys. Z.* **1916**, *17*, 557. (b) $k_d = 4\pi N_A \delta(2D_{phys})/10^3$, where N_A is Avogadro's number.

(20) $k_{ex} = 7.8 \times 10^{10} \exp(-5.35 \times 10^3/RT)$. The preexponential data and activation energy are adopted from Nielson, R. M.; McManis, G. E.; Sanford, L. K.; Weaver, M. J. *J. Phys. Chem.* **1989**, *93*, 2152.

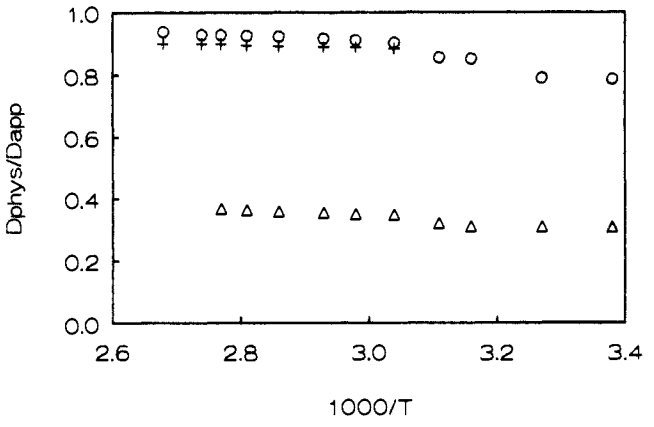

Figure 6. Dependence of D_{phys}/D_{app} on temperature for 53 mM ferrocene in $Me_2PEG/LiClO_4$ (O), pure Fc-MePEG/$LiClO_4$ (Δ), and 42 mM Fc-MePEG in $Me_2PEG/LiClO_4$ (+).

contribution to the overall transport, D_{phys}/D_{app}, for monomer (O) and polymer (+) ferrocene, Figure 6. These results show that (i) electron self-exchange plays a relatively minor (ca. 10%) and nearly identical role in the diffusion coefficient of ferrocene monomer and of Fc-MePEG at temperatures above T_m, and (ii) D_{phys}/D_{app} is, in contrast to the strong temperature dependence of D_{app} on temperature, nearly insensitive to temperature. Further inspection of the calculation shows that D_{phys}/D_{app} is actually not very sensitive to the assumed value of k_{ex} because the magnitude of $[1/k_d + 1/k_{ex}]^{-1}$ is dominated more by k_d (which is in turn determined by D_{phys}) than by k_{ex}. That is, *the electron-hopping contribution is controlled by the collision rate* through D_{phys}.[21]

Calculation of D_{phys}/D_{app} for undiluted Fc-MePEG on the same basis as the above, Figure 6 (Δ), suggests that electron self-exchange might be appreciable[22] in this material. Figure 5 (inset, compare + and Δ) shows, on the other hand, that the *net* value of D_{app} in undiluted Fc-MePEG *decreases* slightly rather than increasing as eq 3 would predict. It is possible that the anticipated increase in the second term in eq 3 is offset by a decrease in D_{phys}, but we think it more likely that k_{ex} for ferrocene electron self-exchange in the polymer melt is actually much smaller than the acetonitrile-derived k_{ex} value[23] used in the calculation, so that the Figure 6 calculations generally *over*estimate the extent of the electron exchange and *under*estimate D_{phys}/D_{app}. It has been shown that electron self-exchanges are slowed in viscous media,[23] and we have measurements in hand[24] demonstrating depressions of electron transfers of $[Fe(phen)_3]^{3+/2+}$ complexes at metal complex polymer interfaces and of $[Co(bpy)_3]^{3+/2+}$ at electrode surfaces when studying couples in Me_2PEG polymer solvents.

The conclusion that we draw from the above considerations is that electron hopping is not a significant contribution to D_{app} for ferrocene monomer and probably not for Fc-MePEG in the polymer solvents.

We should remark on the dimensional aspects of electrochemical measurement of polymer self-diffusion. A proper measure of polymer self-diffusion requires[8] transport of it as a unit, moving its center-of-mass over a distance much larger than the polymer radius of gyration, R_g. In electrochemical terms, the required diffusional distance, d, is connected[14] to the self-diffusion coefficient and the experimental time scale t_{exp} by the relation $d^2 = Dt_{exp}$. The condition $d \gg R_g$ can in principle be met by choice of experimental time scale. In reference to $D_{Fc\text{-}MePEG}$ values at temperature $T > T_m$ in Figure 5, the time scales of voltage scans

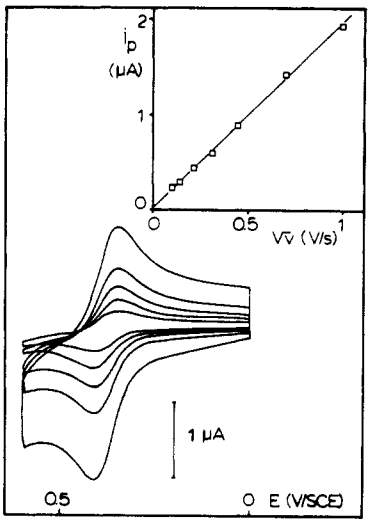

Figure 7. Cyclic voltammetry of a solution of Fc-MePEG **5** (ca. 5×10^{-4} M) in 0.1 M Et_4NClO_4–H_2O at different scan rates, 20, 50, 100, 200, 500, 1000 mV/s at a 1-mm diameter platinum disk. Inset: dependence of the peak current on the square root of scan rate v.

as in Figure 4 are ca. 100 s, so that d is ca. 10^{-3} cm (for $D_{Fc\text{-}MePEG} = 10^{-8}$ cm^2/s), much larger than the fully extended polymer chain dimension of ca. 20 nm. Clearly this condition satisfies the center-of-mass requirement. At room temperature, where $D_{Fc\text{-}MePEG} = 3.9 \times 10^{-12}$ cm^2/s, the currents followed the Cottrell chronoamperometric relation over experimental times of 30–100 s, so $d \approx 110$ to 200 nm, which is still much larger than R_g. Again the center-of-mass requirement is satisfied but by an obviously narrower margin.

It is interesting to contemplate the consequences of encountering even slower diffusion, or using shorter t_{exp}, than the room-temperature $D_{Fc\text{-}MePEG}$ experiment. For example, for $R_g \sim 10$ nm, if $D \sim 1 \times 10^{-12}$ cm^2/s and $t_{exp} \sim 1$ s, then $d \sim R_g$. In this situation, the diffusion quantity is neither a center-of-mass motion nor a bulk polymer property but rather the diffusive mobility of a polymer molecule within, crudely, *the outermost monolayer of molecules of the polymer sample*. That is, only a "monolayer" of the redox sites in the polymer is consumed during the experiment. This estimate shows how electrochemistry is, potentially, sensitive to polymer *surface composition and dynamics* and that conditions may be encountered where Fickian diffusion theory becomes no longer appropriate. Additionally, when the polymeric material is partly crystalline (as with Fc-MePEG at room temperture), analysis of such "monolayer" reactions potentially sheds light on whether the surface ordering differs from that of the bulk or not.

Finally, we should note that the very short diffusion pathlength for undiluted Fc-MePEG at room temperature means that strictly speaking, the microscopic (rather than geometrical) area of the Pt microdisk should be used in the diffusion equations. In practice, mechanically polished Pt generally has a roughness factor of less than 2, and so the maximum error in D_{app} would be of this magnitude.

Electrochemistry of Fluid Polymer Solutions. The electrochemistry of aqueous, CH_3CN, and CH_2Cl_2 solutions of Fc-MePEG provides useful evidence about polymer purity and its diffusion rates in fluid media. The well-defined (macroelectrode) cyclic voltammetry in Figure 7 is typical. The absence of multiple oxidation waves confirms the absence of small amounts of unlabeled ferrocene carboxylic acid, which in water has a larger diffusion coefficient and a formal potential more positive by 170 mV Table II) and which would be readily seen superimposed on the Fc-MePEG response.

Exhaustive electrolyses of Fc-MePEG solutions in 0.1 M Bu_4NPF_6/CH_3CN required electrolysis times longer by 4–5 times than for monomer ferrocene because of the small diffusion coefficient of the polymer in its solutions (vide infra), but log(i) vs t is linear as expected[14] for a chemically uncomplicated redox

(21) This means in turn that we are unlikely to have *over*estimated D_{phys}/D_{app} in the comparison (0,+) in Figure 6 as a result of having assumed a literature[19] k_{ex} determined in acetonitrile or of having assumed the same k_{ex} for Fc-MePEG and for monomer ferrocene in Me_2PEG.

(22) The prediction is mainly a consequence of the larger (10-fold) concentration of ferrocene sites in undiluted Fc-MePEG; that is, in the calculation k_{app} is still nearly diffusion controlled and determined mainly by k_d and D_{phys}.

(23) Zhang, X.; Yang, H.; Bard, A. J. *J. Am. Chem. Soc.* **1987**, *109*, 1916.

(24) Zhang, H.; Longmire, M. L.; Murray, R. W. University of North Carolina, unpublished work, 1988.

Table II. Cyclic Voltammetry Data at a 1-mm Diameter Platinum Disk Electrode for Solutions of Fc-MePEG and Ferrocene

sample and condition		E°,[a]	ΔE_p,[b] range	D[c]
		CH_3CN[d]		
ferrocene				
ref 14		0.0	60–80	2.4×10^{-5}
present work		0.0	65–70	$2.2 (\pm 0.4) \times 10^{-5}$
Fc-$CONH_2$				
ref 25		0.22		
Fc-MePEG				
0.1 M Bu_4NPF_6	dry	0.16	60–75	$3.1 (\pm 0.4) \times 10^{-6}$
	wet[d]	0.16	60–70	$3.1 (\pm 0.4) \times 10^{-6}$
0.1 M $LiClO_4$	dry	0.23	80–100	$3.1 (\pm 0.4) \times 10^{-6}$
	wet[d]	0.23	60–80	$3.1 (\pm 0.4) \times 10^{-6}$
		CH_2Cl_2/0.1 M Bu_4NPF_6		
ferrocene				
		0.0	80–115	$2 (\pm 0.3) \times 10^{-5}$
Fc-MePEG				
	dry	0.14	80–135	$1.7 (\pm 0.4) \times 10^{-6}$
	wet[d]	0.15	70–80	$2.3 (\pm 0.4) \times 10^{-6}$
		H_2O		
Fe-COO^-, Na^+				
0.1 M Et_4NClO_4		0.55	115–140	$4.3 (\pm 0.6) \times 10^{-6}$
0.1 M $LiClO_4$		0.55	115–120	$4.2 (\pm 0.6) \times 10^{-6}$
Fc-MePEG				
0.1 M Et_4NClO_4		0.38	60–65	$3.1 (\pm 0.5) \times 10^{-6}$
0.1 M $LiClO_4$		0.38	70–85	$3.1 (\pm 0.5) \times 10^{-6}$

[a] V vs SCE in water, vs Fc^+/Fc in nonaqueous media. [b] Peak-to-peak separation, mV, measured for scan rates v, $0.02 < v < 1$ V/s. [c] D, cm^2/s, calculated from the peak currents.[14] [d] Ca. 1 ppt H_2O.

conversion. The coulometric charges for electrolysis of solutions containing known weights of Fc-MePEG gave values of $n = 1.2 \pm 0.1$ electrons per molecule, by using MW = 2590 for the Fc-MePEG. This result is in satisfactory agreement with the ideal $n = 1.0$, given the difficulty of properly correcting for small background currents flowing during the lengthy electrolyses.

In the cyclic voltammetry of Figure 7, the ratio of oxidation and reduction peak currents is close to unity, and the oxidation peak current i_p varies linearly with $v^{1/2}$ (see inset), criteria[14] demonstrating a diffusion-controlled, chemically reversible reaction of the ferrocene moiety of the monotagged poly(ether) chain. Results calculated[14] for diffusion coefficients of Fc-MePEG polymer and of ferrocene monomers in the various media are given in Table II for H_2O and for carefully anhydrous and moist CH_3CN and CH_2Cl_2. There are no effects of trace water or of using lithium vs tetraalkylammonium electrolytes.

In CH_3CN and CH_2Cl_2, the ferrocene-labeled polymer diffuses about 10× more slowly than does monomer ferrocene. (In water, the difference is less, but there we had to use (for solubility reasons) the ferrocene carboxylate anion, and we regard this comparison as less meaningful.) The nonaqueous results were examined by using the expression[26]

$$D_P = D_M(M_{mono}/M_{poly})^m \quad (4)$$

where D_P and M_{poly} are the diffusion coefficient and MW of the polymer, respectively, and D_M and M_{mono} are those quantities for the monomer unit of the polymer. The power m is generally 0.55 in a good solvent, assuming random spherical coiling of the polymer.[26] Not knowing D_M for the $-CH_2-CH_2-O-$ monomer unit, we approximate it with the diffusion coefficient measured for the ferrocene monomer in the given solvent (Table II). Taking $M_{mono} = 44$ and $M_{poly} = 2590$, eq 4 gives $m = 0.5$ and 0.6 in CH_3CN and CH_2Cl_2, respectively, values which are consistent with the model of random spherical coiling of the labeled polymer.

That m is larger for CH_3CN than CH_2Cl_2 (shown by comparing D_P/D_M values, with no approximation) is also consistent with expectations about solvation of poly(ether) chains; CH_2Cl_2 is a good poly(ether) solvent giving an expanded, more slowly diffusing coil, whereas CH_3CN is a poorer solvent (being the basis of some PEO θ solvent mixtures[27]) and gives a more shrunken, faster coil.

Lastly, cyclic voltammetric peak potential separations (Table II), ΔE_p, potentially reveal kinetic effects of the polymer chain appendage on the ferrocene heterogeneous electron-transfer dynamics. The polymer and monomer ferrocene voltammetry were compared, in order to account for increase in ΔE_P due to uncompensated resistance, a known problem in the ΔE_P method.[28,29] The large ΔE_P in dry CH_2Cl_2 and CH_3CN for Fc-MePEG and ferrocene became smaller after adding trace water and are for both ferrocenes plausibly taken as simply iR effects of increased medium ionic conductivity in the wet media. Whatever electron-transfer kinetic effects exist in the nonaqueous environments are of smaller and unobservable magnitude. The aqueous results reveal a possible electron-transfer kinetic effect. The polymer ΔE_P is *smaller* than for ferrocene carboxylate; that is, the polymer heterogeneous kinetics appear to be accelerated compared to the monomer. This interesting result requires a more demanding kinetics analysis, including inspection for adsorption or other surface effects, before any chemical interpretation can be offered.

Experimental Section

Chemicals. Reagents were as follows: methoxy poly(ethylene glycol) (MePEG, Polysciences, nominal MW 1900); poly(ethylene glycol) dimethyl ether (Me_2PEG, Polysciences, nominal MW 2000); thionyl chloride (Fisher, distilled before use); toluene (Fisher); DMF, acetonitrile, and methylene chloride (Burdick and Jackson, spectrochemical grade, stored over 4-Å molecular sieves); alumina (Fisher, 80–200 mesh, activated overnight at 300 °C); $LiClO_4$ (Aldrich), Et_4NClO_4 and Bu_4NPF_6 (Fluka, recrystallized and dried by heating under vacuum).

Measurements. ^{13}C NMR (100.563 MHz) spectra were obtained in $CDCl_3$ with a Varian XL-400 and IR spectra with a Nicolet D30 FT-IR. Differential scanning calorimetry was performed under N_2 on a Perkin-Elmer DSC-4 with polymer samples that were scanned (20 °C/min) and uniformly cooled. Elemental analysis was by Galbraith Labs (Knoxville, TN). Gel permeation chromatography was done at 23 °C with a Waters GPC-244 chromatograph equipped with RI and UV–vis detectors, with tetrahydrofuran as carrier solvent (1 mL/min) in TSK-GEL $G4000H_{XL}$, $G\text{-}3000H_{XL}$ and $G2000H_{XL}$ (Toso) columns that had been calibrated with narrow-distribution poly(ethylene glycols) (10 samples of MW = 1.06×10^2 to 4.00×10^4, from Toso). Samples (0.3 mL) were injected at concentrations of 0.2% (wt/vol).

Electrochemistry of ca. 1-mL fluid solutions was done with a 1-mm diameter Pt disk working electrode in a frit-divided three-compartment cell in an inert atmosphere glovebox in the nonaqueous cases.

Solid-state polymer voltammetry was carried out with a previously described[3] microelectrode-based cell consisting of the tips of 10 μm diameter Pt, 0.38 mm diameter Pt, and 0.38 mm diameter Ag wires (as working, auxiliary, and reference electrodes, respectively). The Pt microelectrode was sealed in a glass capillary which was potted with the other electrodes in a cylinder of epoxy resin (Miller-Stephenson Chemical); the end of the cylinder is polished flat to expose the three wire tips. Solid-state voltammetry was done on three types of polymer samples: purified, undiluted ferrocene-labeled Fc-MePEG ($C_{Fc\text{-}MePEG} = 0.43$ M), ferrocene-labeled Fc-MePEG diluted (to $C_{Fc\text{-}MePEG} = 42$ mM) with poly(ethylene glycol) dimethyl ether (Me_2PEG-2000), and ferrocene dissolved (at $C_{Fc} = 53$ mM) in Me_2PEG-2000. $LiClO_4$ electrolyte was added in a ratio (ether oxygen)/Li = 16. The polymer mixtures were melted and dried at 65 °C in thin glass tubes in a vacuum oven for 10 h, after which the cylindrical microelectrode assembly was inserted into the polymer melt and sealed with Teflon tape. The polymers were cooled to room temperature and stored at least 24 h before the voltammetry.

MePEG-Cl [$CH_3O(CH_2CH_2O)_nCH_2CH_2Cl$], 2. A 250-mL, three-necked, round-bottomed flask charged with 19.0 g MePEG (**1**) and 100 mL of toluene was heated at vigorous reflux, discarding the first 30 mL of toluene/water azeotrope collected in the Dean-Stark trap and transferring the next 20 mL of dry toluene from the trap to a dropping funnel along with 2.2 mL (30 mmol) of freshly distilled $SOCl_2$. Replacing the trap with a condenser, 1.0 mL (10 mmol) of DMF catalyst (freshly dried over ca. 1 g activated alumina) is added to the reaction flask. DMF is

(25) Little, W. F.; Reilley, C. N.; Johnson, J. D.; Sanders, A. P. *J. Am. Chem. Soc.* **1964**, *86*, 1382.

(26) (a) Tanford, C. *The Physical Chemistry of Macromolecules*; Wiley: New York, 1961; Chapter 6. (b) Saji, T.; Pasch, N. F.; Webber, S. E.; Bard, A. J. *J. Phys. Chem.* **1978**, *82*, 1101.

(27) Brandrup, J.; Immergut, E. H. *Polymer Handbook*, 2nd ed.; Wiley: New York, 1975; Chapter IV-7.

used instead of pyridine[1] which others have implicated in PEG decomposition.[30] The pale yellow $SOCl_2$/toluene solution is slowly added over ca. 20 min to the stirred MePEG/toluene solution, and after a 2-h reflux the crude MePEG-Cl (**2**) solution is reduced to a viscous melt at reduced pressure in a rotary evaporator. Taking up the brownish polymer in 150 mL of dried (K_2CO_3) CH_2Cl_2, the solution was filtered, degassed with Ar, treated with 50 g of activated alumina in a 500-mL flask for 30 min to remove traces of $SOCl_2$, filtered, and reduced to 30 mL, 150 mL of ether was added, and the solution was cooled in the freezer for 2 h after which 15.1 g (yield 79%) of off-white powder MePEG-Cl (**2**) was collected: IR (KBr pellet) 1110 cm^{-1} (CH_2OCH_2), 669 cm^{-1} (CCl) and no detectable OH absorption at 3300–3500 cm^{-1}.

MePEG-N_3[$CH_3O(CH_2CH_2O)_nCH_2CH_2N_3$], 3. NaN_3 (3.3 g, 51 mmol) was added with stirring to 12 g (6.3 mmol) of MePEG-Cl (**2**) in 100 mL of DMF (dried over 4 Å molecular sieves and freshly vacuum distilled[31]) heated under Ar to 120 °C (oil bath) in a flask equipped with reflux condenser. After stirring at 120 °C for 4 h, the solution was cooled to room temperature and filtered, the DMF was removed under reduced pressure in a rotary evaporator, the viscous polymer melt was taken up in 50 mL of CH_2Cl_2, and filtered, 150 mL of ether was added, and the solution was cooled in the freezer for 2 h. The collected precipitate was reprecipitated once further and 11 g (92% yield) of MePEG-N_3 (**3**) was collected as an off-white power: IR (KBr pellet) 2108 cm^{-1} (N_3^-), 1110 cm^{-1} (CH_2OCH_2), and no absorption for Cl at 669 cm^{-1}.

MePEG-$NH_3^+Cl^-$, [$CH_3O(CH_2CH_2O)_nCH_2CH_2NH_3^+Cl^-$], 4. MePEG-$N_3$ (**3**) (10.0 g, 5.3 mmol), 60 mL of absolute EtOH, and 20 mL of CH_2Cl_2 purged with Ar in a Parr bottle, to which 1.5 g of 5% Pd(C) was added, hydrogenated overnight at 50 psi H_2. The product solution was filtered through Celite and then through a 0.45-μm syringe filter (Gelman Sciences) to remove residual catalyst, and the solvent was pumped off. The crude product was taken up in 20 mL of CH_2Cl_2 and 100 mL of ether and was chilled in the freezer for 2 h; the precipitate was collected and reprecipitated to yield 7.5 g (75%) of a white powder: IR (KBr pellet) 3300 cm^{-1} (NH_3^+), 1110 cm^{-1} (CH_2OCH_2), and no absorption for N_3 at 2108 cm^{-1}.

Fc-MePEG, [$CH_3O(CH_2CH_2O)_nCH_2CH_2NH(CO)CpFeCp$], 5. MePEG-$NH_3^+Cl^-$ (**4**) (0.95 g, 0.5 mmol), 0.12 g (0.5 mmol) of ferrocene carboxylic acid, 0.07 g (0.5 mmol) of 1-hydroxybenzotriazole, 0.12 g (0.6 mmol) of dicyclohexylcarbodiimide, 0.14 mL (1.0 mmol) of triethylamine, and 50 mL of CH_2Cl_2 in a sealed flask were stirred in the dark for 5 days and filtered. Ether was added after standing in the freezer for 2 h, and 0.84 g of crude Fc-MePEG (**5**) was collected. This product, dissolved in 2.0 mL of water was centrifuged to remove an insoluble white material and subjected to chromatography on a 1.7 × 20 cm phenyl-sepharose (Pharmaceia, CL-4B) column, eluting with 0.5 M $(NH_4)_2SO_4$. (This gel column was stored in 20% EtOH, after washing, in order, with 100 mL each of 0.5 M $(NH_4)_2SO_4$, distilled H_2O, and 20% EtOH and was prepared for use by the reverse of this procedure.) The single orange-colored band was collected, extracted with CH_2Cl_2 (3 × 10 mL), precipitated with ether, and dried in a vacuum desiccator at room temperature for 24 h to yield 0.50 g (53% yield; 29% yield overall MePEG) of pale orange powder Fc-MePEG (**5**): IR 1649 cm^{-1} (C–O, amide), 1110 cm^{-1} (CH_2OCH_2), no absorption for NH_2 at 3324 cm^{-1}; ^{13}C NMR (100.6 MHz, $CDCl_3$) 38.4, 58.2, 67.6, 69.7, 75.9, 76.2, 76.4 ppm. Elemental anal. Calcd for [$CH_3O(CH_2CH_2O)_{52.4}CH_2CH_2NH(CO)$-$CpFeCp$] ($C_{118.8}H_{226.6}Fe_1N_1$): C, 55.09; H, 8.78, N, 0.54; Fe, 2.16. Found: C, 55.10; H, 8.56; N, 0.63; Fe, 1.86.

Acknowledgment. Y.L.M. acknowledges with gratitude a NATO Fellowship. The research was supported in part by grants from the Department of Energy (DE-FG05-87ER13675) and the National Science Foundation.

(28) Nicholson, R. S. *Anal. Chem.* **1965**, *37*, 1351.
(29) (a) Bond, A. M.; Henderson, T. L. E.; Mann, D. R.; Mann, T. F.; Thormann, W.; Zoski, C. G. *Anal. Chem.* **1988**, *60*, 1878. (b) Kadish, K. M.; Ding, J. Q.; Malinski, T. *Anal. Chem.* **1984**, *56*, 1741.
(30) (a) Harris, J. M.; Yalpani, M.; Van Alstine, J. M.; Struck, E. C.; Case, M. G.; Paley, M. S.; Brooks, D. E. *J. Polym. Sci., Polym. Ed.* **1984**, *22*, 341. (b) Harris, J. M.; Hundley, N. H.; Shannon, T. G.; Struck, E. C. *J. Org. Chem.* **1982**, *47*, 4789.
(31) Perrin, D. D.; Armagero, W. L. F.; Perrin, D. R. *Purification of Laboratory Chemicals*, 2nd ed.; Pergamon Press: New York, 1980.

The Effect of Pressure on the Surface Plasmon Absorption Spectra of Colloidal Gold and Silver Particles

Jeffery L. Coffer, John R. Shapley,* and Harry G. Drickamer*

Contribution from the School of Chemical Sciences, Department of Physics, and Materials Research Laboratory, University of Illinois, Urbana—Champaign, Urbana, Illinois 61801.
Received December 19, 1989

Abstract: The first measurements of the effect of pressure on the peak position (ω_{sp}) and line width (fwhm) of the surface plasmon absorption in several Au and Ag hydrosols have been recorded up to 10 kbar. Red shifts of the plasmon peak with increasing pressure are observed for relatively large metal particles prepared by the citrate procedure (Au, $\bar{d}$ = 265 Å; Ag, $\bar{d}$ = 230 Å). The shift for silver is over twice that of gold (−420 cm^{-1} vs −200 cm^{-1}). These red shifts are interpreted in terms of pressure-induced volume changes within the context of a free-electron model. In contrast, particles prepared by the Faraday method (Au, $\bar{d}$ = 54 Å; Ag, $\bar{d}$ = 60 Å) show initial blue shifts with pressure, with the magnitude again larger for silver. Upon aging (as well as upon heating in the case of Au), the Au and Ag Faraday sols exhibit an increase in their average particle size and degree of aggregation. Correspondingly, the pressure response of their plasmon absorption approaches that of the citrate sols.

Interest in the physicochemical properties of colloidal metal particles has been ongoing since the time of Faraday, who demonstrated that colloidal gold particles can be formed in a facile manner by reduction of an aqueous gold salt solution with white phosphorus.[1] Current efforts focus on a number of different areas and applications. One is the area of catalysis, where workers have investigated the reactivity of colloidal metal particles on oxide supports[2] as well as implicated metal colloids as the active species in a number of reactions previously thought to be homogeneously catalyzed.[3] Additional studies have also examined colloidal metal particles for applications as biological stains[4] and ferrofluids.[5] On a fundamental level, the issue of "quantum size effects" is an

(1) Faraday, M. *Philos. Trans.* **1857**, *147*, 145.
(2) (a) Bradley, J. S.; Leonowicz, M. E.; Witzke, H. *J. Mol. Catal.* **1987**, *41*, 59. (b) Thomas, J. M. *Pure Appl. Chem.* **1988**, *60*, 1517.
(3) (a) Lewis, L. N.; Lewis, N. *J. Am. Chem. Soc.* **1986**, *108*, 7228. (b) Lewis, L. N.; Lewis, N. *J. Am. Chem. Soc.* **1986**, *108*, 743. (c) Picard, J. P.; Dunogues, J.; Elyussfi, A. *Synth. Commun.* **1984**, *14*, 95. (d) Freeman, F.; Kappos, J. C. *J. Am. Chem. Soc.* **1985**, *107*, 6628. (e) Maier, W. F.; Chettle, S. J.; Rai, R. S.; Thomas, G. *J. Am. Chem. Soc.* **1986**, *108*, 2608. (f) Burk, P. L.; Pruett, R. L.; Campo, K. S. *J. Mol. Catal.* **1985**, *33*, 1.
(4) (a) Faulk, W.; Taylor, G. *Immunochem.* **1971**, *8*, 1081. (b) Roth, J.; Bendayan, M.; Orci, L. *J. Histochem. Cytochem.* **1980**, *28*, 55.
(5) Charles, S. C.; Popplewell, J. In *Ferromagnetic Materials*; Wohlharth, E. P., Ed.; North Holland: Amsterdam, 1980; Vol. 2.

0002-7863/90/1512-3736$02.50/0